Intra-datacenter Optical Circuit Switch Architecture with Multi-band Transmission Technologies

Takuma Kuno, Reiji Higuchi, Kazato Satake, Hayato Yuasa, Yojiro Mori, Hiroshi Hasegawa
Nagoya University, Furo-cho, Chikusa, Nagoya, 464-8603 Japan
kuno.takuma.g2@s.mail.nagoya-u.ac.jp

Abstract: This paper proposes an optical circuit switch architecture using multi-band transmission. We experimentally confirmed the performance of 1,280×1,280 switch with 32-Gbaud dual-polarization QPSK signals aligned on 33-GHz grid in the C- and L- bands. © 2024 The Authors

1. Introduction

Traffic demands related to datacenters are exploding, and the total amount of intra-datacenter traffic is about five times that of IP traffic. Traditional datacenters employ electrical switches to connect top-of-rack switches while the transmission links have been opticalized [1]. This typical setup consumes a lot of power because the electrical switching requires a large number of optical-to-electrical and electrical-to-optical convertors. To address this issue, optical and electrical hybrid switch network architectures and fully optical switch network architectures are being extensively studied [2-5]. These approaches can reduce the power consumption of datacenter networks by replacing the electrical switches with optical circuit switches. Google reported that they had already installed 136×136 optical circuit switches in their intra-datacenter networks for switching the traffic in the spine layer of the multi-tier topology [6].

To process a large amount of intra-datacenter traffic more cost-effectively, optical circuit switches must have high port counts and high throughputs. High-port-count and high-throughput optical circuit switches realize single-hop switching networks which eliminates multi-stage switching and simplifies both fiber interconnection and traffic control [7]. So far, extensive research has been conducted on various optical circuit switch architectures [6-14]. Among them, the combination of delivery-and-coupling (DC) space switches and wavelength-routing (WR) switches consisting of optical couplers and arrayed-waveguide gratings (AWGs) is a promising candidate for intra-datacenter interconnection [12-14]. By connecting WR switches in parallel with DC space switches, the total port count of the entire switch reaches the product of the port counts of the sub-switches. Moreover, the wavelength-division multiplexing offered by the WR switches can reduce costs as multiple wavelength signals can share optical devices. To increase the switch throughput further, we need to expand the bandwidth of the WR switches. However, the loss of the optical couplers in the WR switch increases with the number of wavelength channels. In addition, the center frequencies of AWG passbands deviate significantly from the defined grid with the expansion of the available bandwidth [14]. This yields contention and signal quality degradation.

In this paper, we propose a novel optical circuit switch architecture that uses multi-band transmission technology. By introducing the super-channel configuration, bitrate per port can be cost-effectively increased while restraining the WR switch loss. In addition, WR switches are newly configured with optical couplers and selectors to route signals without contention and quality degradation. Proof-of-concept experiments confirm the feasibility of a 1,280×1,280 switch processing 20-wavelength 9.8 Tbps signals consisting of 14-wavelength and 7-spatial sub-channels, where each sub-channel is a 32-Gbaud dual-polarization (DP) QPSK signal on a 33-GHz grid in the C- and L- bands.

2. Proposed Switch Architecture

Figure 1(a) illustrates the basic switch architecture using DC space switches and WR switches [12-14]. The switch consists of MN wavelength-tunable transmitters supporting N wavelengths and S spatial sub-channels, SN $M\times M$ DC space switches comprising M $1\times M$ optical selectors and M $M\times 1$ optical couplers, SM $N\times N$ WR switches, and MN receivers supporting S spatial sub-channels, where N and M represent the number of wavelengths and the port count of the DC switch, respectively. Figure 1(b) shows the previously proposed WR switch. The WR switch consists of n $N/n\times 1$ optical couplers, n optical amplifiers, n 1×2 splitters, and a pair of $n\times N/2$ uniform-loss and cyclic frequency (ULCF) AWGs [13]. The WR switch can handle Nyquist WDM signals; thanks to a pair of AWGs whose passbands are interleaved, the WR switch has enough passband bandwidth to demultiplex Nyquist WDM signals.

The switch throughput is given by $SMEB$, where S, M, E, and B denote the number of spatial sub-channels, the DC space switch port count, spectrum efficiency of WR switches, and the available bandwidth of WR switches, respectively. To increase the switch throughput further, these four design parameters need to be increased. However,

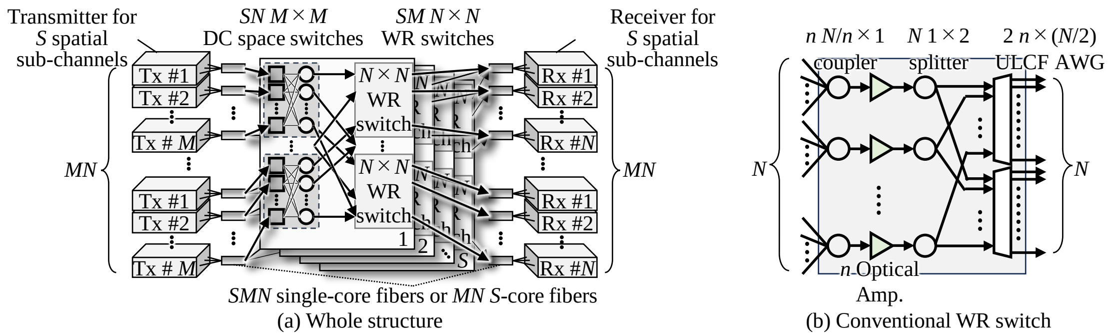

Fig. 1. Optical switch architecture consisting of DC space switches and WR switches.

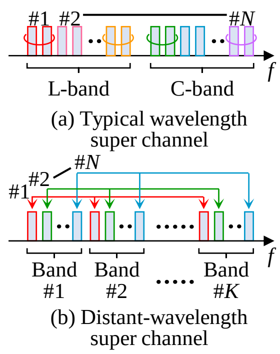

Fig. 2. Wavelength super-channel configuration.

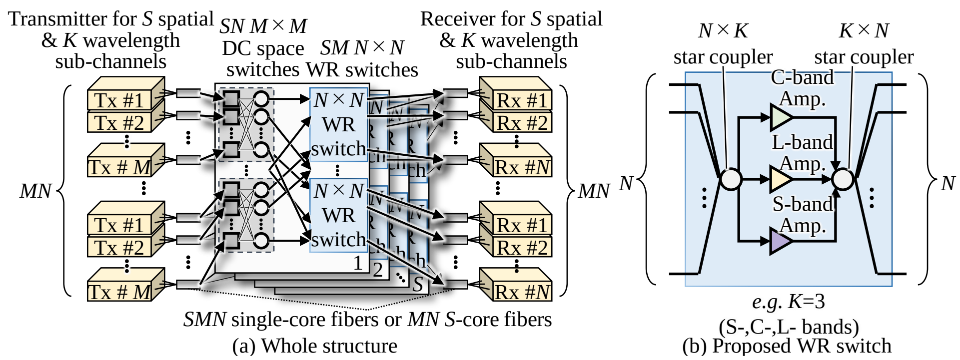

Fig. 3. Proposed switch architecture.

the number of spatial sub-channels, S, is limited by the number of available cores in a cable. Expansion of the DC space switch port count, M, is infeasible because the insertion loss of the DC space switch increases with its port count. Spectrum efficiency, E, has already become saturated with the use of Nyquist WDM. Thus, the available bandwidth of WR switch, B, must be extended to increase the switch throughput. However, the loss in the aggregation coupler in the WR switch increases with the number of wavelength channels. The use of wavelength super-channels can increase the bitrate per channel without increasing the coupler loss by using multiple wavelength sub-channels as a channel as shown in Fig. 2(a). However, the typical wavelength super-channel scheme increases transponder cost because all transponder lasers must support the broader wavelength range. Moreover, the center frequency of AWG passbands can deviate significant from the defined grid as the bandwidth is expanded. This causes contention and signal quality degradation.

To reduce transponder cost for multi-band transmission, we employ a novel super-channel configuration, namely the distant-wavelength super-channel. Figure 2(b) shows its concept. In this scheme, the total available band is divided into K bands, where each band has N wavelength signals. A wavelength super-channel is formed with one sub-channel in each of the K bands. Therefore, each laser does not have to support the entire wavelength range. Figures 3(a) and (b) show the newly proposed optical circuit switch and WR switch, respectively. The K wavelength sub-channels share the fiber and DC switch connecting the transmitter/receiver and the switch. The WR switch consists of N×K star coupler, K optical amplifiers, K×N star coupler, where K is the number of bands. By using optical couplers instead of AWGs, the proposed WR switch is free from the center frequency deviation problem, which enables us to use signals in different bands without contention and signal quality degradation. In addition, the switch loss can be kept constant when the number of bands, K, is under N/n. Although channels on different wavelength bands exist in the output of star couplers, they are not amplified at the subsequent EDFAs. In addition, because this configuration assumes the use of a coherent system, undesired wavelength channels can be eliminated at the receiver by optical, analog, and digital filtering.

3. Experiments

We conducted experiments to evaluate the performance of our optical switch architecture. Figure 4 shows the experimental setup. At the transmitter side, three continuous waves (CW) in the C- or L-bands were generated by three tunable lasers, where CW center frequencies were separated by 33 GHz. 32-Gbaud QPSK signals were created by a lithium-niobate IQ modulator driven by an arbitrary-waveform generator. Next, a dual-polarization signal was created by a polarization-division multiplexing (PDM) emulator consisting of polarization-beam splitter, a delay fiber, and a polarization-beam combiner (PBC); this yielded quasi-Nyquist WDM 32-baud DP-QPSK signals, where the center channel was used as the target channel. The signals of distant-wavelength super channels corresponding to the target signals were created in the same manner as the target channel. Note that, when the target channel was on the edge of C- and L-bands, two signals and their corresponding distant-wavelength super channels were created. After the signal power was controlled by EDFAs, the signals were combined and split by 2×2 optical coupler. One tributary was split into eight tributaries by a 1×8 splitter, where seven of the tributaries were input to a 1-km 7-core fiber. The other tributaries were used to generate inter-core crosstalk in the multi-core fibers and intra-band crosstalk of DC space switch. Power of each signal was set to 2 dBm. The loss of the 7-core fiber was 2 dB; this included the fan-in and fan-out losses. After passing through the 7-core fiber, the target signal was input to the switch under the test. Here, we constructed a part of a 1,280×1,280 optical circuit switch, where DC-switch scale *M* was 64. The measured DC space switch loss was 21 dB. The intra-band crosstalk was injected to the egress optical couplers, where the extinction ratio of the selector was around 35 dB. We used a WR switch configuration that combined 20×2 star couplers, C-band EDFA, L-band EDFA, and 2×20 star couplers. The measured losses of 20×2 star couplers and 2×20 star couplers were 13.7 dB and 13.3 dB, respectively. As inter-band crosstalk, ASE noise was combined with the target signal with its adjacent signals via a 20×2 star coupler, where the band for the target and its adjacent channels were eliminated by a wave shaper. After passing through a 1-km 7-core fiber, the target signal was detected by a digital coherent receiver including a pre-filter and a pre-amplifier.

Fig. 5 plots the measured BERs versus wavelength sub-channel numbers. Considering the worst case in terms of inter-core crosstalk, we evaluated signals of the central core in the 7-core fiber. There was a degradation in signal quality in L-bands, due to the noise figure of EDFAs used. Nevertheless, we confirmed that all BERs were under the target value of 10^{-2}. The total throughput of the switch prototype was 12.54 Pbps (=20×9.8 Tbps×64).

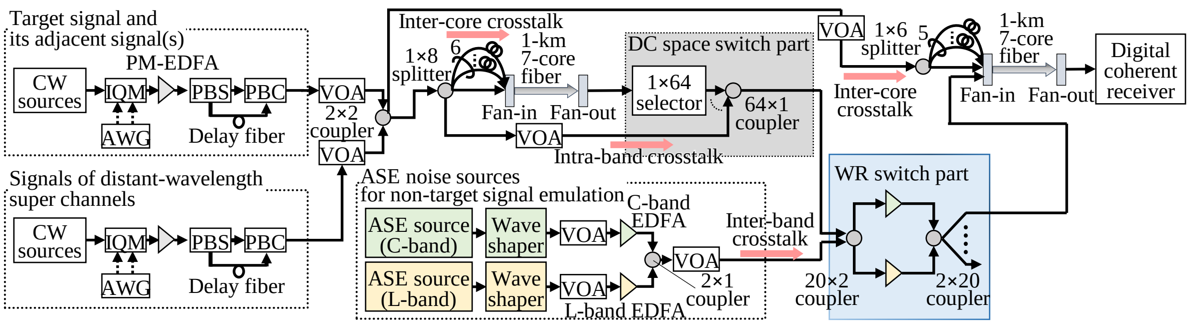

Fig. 4. Experimental setup.

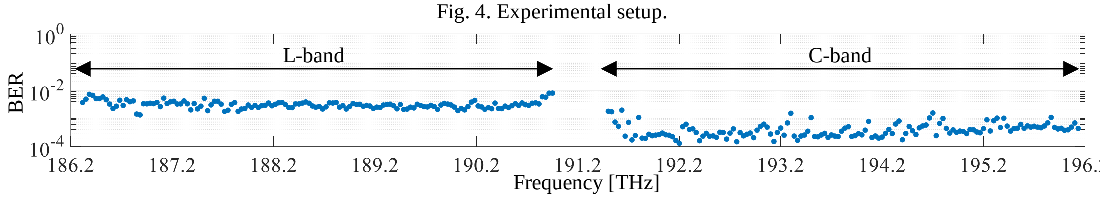

Fig. 5. Experimental results.

4. Conclusion

We confirmed the feasibility of the proposed optical circuit switch that exploits multi-band transmission technologies. We measured the BERs of 9.8 Tbps DP-QPSK signals comprising wavelength sub-channels and spatial sub-channels, where each sub-channel was a 32-Gbaud DP-QPSK signal with 33-GHz bandwidth. The total throughput reached 12.54 Pbps, and the total switch port count was 1,280×1,280.

Acknowledgment: This work was partly supported by JSPS/KAKENHI (JP22J23852) and Foundation of Public Interest of Tatematsu.

5. References

[1] C. Kachris *et al.*, Optical Interconnects for Future Data Center Networks (Springer, 2012).
[2] X. Xue *et al.*, OFC, W1F.5 (2020).
[3] F. Yan *et al.*, IEEE/OSA J. Opt. Commun. Netw. **10**, 1-14 (2018).
[4] K. Sato *et al.*, IEEE Commun. Mag. **51**, 46-52 (2013).
[5] C. Kachris *et al.*, IEEE Commun. Surv. **14**, 1021-1036 (2012).
[6] L. Poutievski *et al.*, ACM SIGCOMM, pp. 66-85 (2022).
[7] K. Sato *et al.*, IEEE/OSA J. Lightw. Technol. **36**, 1411-1419, (2018).
[8] T. J. Seok *et al.*, OSA Optica **6**, 490-494 (2019).
[9] Q. Cheng *et al.*, OSA Photonics Res. **7**, 155-161 (2019).
[10] K. Suzuki *et al.*, IEEE/OSA J. Lightw. Technol. **37**, 116-122 (2018).
[11] M. Ding *et al.*, IEEE J. Sel. Top. Quantum Electron. **24**, 1-8 (2017).
[12] E. Honda *et al.*, OFC, W1F.2 (2020).
[13] H. Nagai *et al.*, IEEE/OSA J. Opt. Commun. Netw. **10**, 82-89 (2018).
[14] T. Kuno *et al.*, OFC, Th3A.2 (2022).